

# $J/\psi$ photoproduction in ultra-peripheral Pb-Pb and p-Pb collisions with the ALICE detector

Jaroslav Adam<sup>1,a</sup>, on behalf of the ALICE Collaboration

<sup>1</sup>Faculty of Nuclear Sciences and Physical Engineering  
Czech Technical University in Prague

**Abstract.** Ultra-relativistic heavy ions generate strong electromagnetic fields which offer the possibility to study gamma-gamma, gamma-nucleus and gamma-proton processes at the LHC in ultra-peripheral Pb-Pb and p-Pb collisions. Exclusive photoproduction of  $J/\psi$  vector mesons is sensitive to the gluon distribution of the target. Here we report on the ALICE measurement of  $J/\psi$  coherent photoproduction in Pb-Pb ultra-peripheral collisions at  $\sqrt{s_{NN}} = 2.76$  TeV for the rapidity ranges  $-3.6 < y < -2.6$  and  $|y| < 0.9$ , and on preliminary results on the  $J/\psi$  photoproduction in p-Pb at  $\sqrt{s_{NN}} = 5.02$  TeV. The  $J/\psi$  mesons have been identified through their leptonic decays.

## 1 Introduction

The photonuclear reactions involving heavy vector meson exclusive production provide a good tool to test the behavior of the gluon distribution functions at low Bjorken- $x$ , because the photoproduction cross section scales at leading order as the square of the gluon PDF. The  $J/\psi$  photoproduction from  $\gamma$ Pb interactions allows to study nuclear gluon shadowing, while the photoproduction reactions from  $\gamma$ p interactions are sensitive to saturation phenomena.

At the LHC it is possible to study photonuclear reactions at higher energies than ever before, via ultra-peripheral collisions (UPC). In these interactions the nuclei or protons are passing each other at a distance greater than the sum of the nuclear radii in the ion-ion case, or at impact parameter large enough to strongly suppress the hadronic interactions in the case of ion-proton system or proton-proton collisions. The physics of ultra-peripheral collisions is reviewed in [1].

As the hadronic interactions are suppressed, the only mechanism in question is via the strong electromagnetic field, whose intensity is proportional to the square of the electric charge of the ion. The electromagnetic field is described as a flux of virtual photons [3],  $dN/dk$ , and the photoproduction cross section is then given by an integration over all photon momenta  $k$ . As a consequence of the proportionality to the square of the electric charge, in Pb-Pb UPC each lead ion is a photon source or a target with equal probability, but in the proton-lead case the lead ion is most likely the photon source.

Exclusive  $J/\psi$  photoproduction has been previously measured in Au-Au collisions at RHIC [4], exclusive  $J/\psi$  photoproduction in  $\gamma$ p interactions has been studied at HERA [5] [6], in  $p\bar{p}$  collisions at Tevatron [7] and recently LHCb reported exclusive  $J/\psi$  and  $\psi(2S)$  production in pp collisions [8].

---

<sup>a</sup>e-mail: jaroslav.adam@cern.ch

The ALICE experiment provided the first LHC measurement on exclusive  $J/\psi$  photoproduction in Pb-Pb collisions at  $\sqrt{s_{NN}} = 2.76$  TeV [9], [10] and now the analysis on  $J/\psi$  photoproduction in p-Pb collisions at  $\sqrt{s_{NN}} = 5.02$  TeV is well advanced and preliminary results are reported below.

## 2 Exclusive photoproduction processes

In terms of perturbative QCD the photonuclear reactions are described in leading order as two-gluon exchange between virtual  $c\bar{c}$  pair created by photon and the target object, which is in our case the proton or the lead nucleus.

In the case of a Pb-Pb UPC two mechanisms for  $J/\psi$  exclusive production may occur. The coherent production is a result of coherent photon coupling to the nucleus, leading to lower values of  $p_T$  of the produced  $J/\psi$  ( $\langle p_T \rangle \sim 1/R_{Pb} \sim 60$  MeV/c). The coupling to a single nucleon is characterized as the incoherent production leaving  $J/\psi$  at relatively higher transverse momenta  $\langle p_T \rangle \sim 1/R_p \sim 500$  MeV/c.

In p-Pb collisions the  $\gamma p$  reactions are dominant and the exclusively produced  $J/\psi$  comes from the collision with the proton. The  $J/\psi$  photoproduction is elastic when the proton does not break nor become excited after the interaction.

Both the Pb-Pb and p-Pb exclusive  $J/\psi$  production is accompanied by the QED process  $\gamma\gamma \rightarrow \mu^+\mu^-$  or  $e^+e^-$ , which is two-photon interaction producing a lepton pair, having thus the same experimental signature as lepton pairs coming from the  $J/\psi$  decays.

## 3 The ALICE experiment at LHC

The ALICE experiment consists of central tracking detectors covering pseudorapidity  $|\eta| < 0.9$ , forward muon spectrometer at rapidity range  $-4.0 < \eta < -2.5$ , forward scintillator arrays on both sides at pseudorapidities  $2.8 < \eta < 5.1$  and  $-3.7 < \eta < -1.7$  and zero degree neutron and proton calorimeters placed on both sides at a distance of  $\pm 116$  meters from the nominal ALICE interaction point.

The central tracking system is composed of the Inner Tracking System (ITS) with 6 layers of position sensitive semiconductor detectors, the two innermost layers of Silicon Pixel Detectors (SPD) have extended pseudorapidity ranges to  $|\eta| < 2.0$  and  $|\eta| < 1.4$ . Surrounding the ITS there is a gaseous tracking detector, Time Projection Chamber (TPC), which serves for tracking and particle identification by specific energy loss measurement. The TPC detector covers the pseudorapidity interval  $|\eta| < 0.9$ . The Time of Flight detector (TOF) is located beyond the TPC. The TOF pseudorapidity coverage is the same as that of the TPC. The central detectors are all placed inside a large solenoid magnet of magnetic field  $B = 0.5$  T.

The muon spectrometer consists of 5 MWPC tracking stations, a dipole magnet creating an integrated field of 3 Tm and a trigger system which can select muon candidates according the transverse momentum using a programmable threshold. A composite absorber is placed in front of the tracking station. The absorber thickness is 10 interaction lengths, enabling thus muon filtering. The pseudorapidity coverage of muon tracking and trigger systems is  $-4.0 < \eta < -2.5$ .

The forward scintillator arrays, VZERO, are used for trigger and event selection. There are two arrays on opposite sides of the nominal interaction point, each composed of 32 scintillator tiles. The VZERO-A is placed at the opposite side of the muon arm at a distance of 340 cm from the interaction point, covering pseudorapidity  $2.8 < \eta < 5.1$ . The VZERO-C as placed at the muon arm side at pseudorapidity  $-3.7 < \eta < -1.7$ , the distance from the interaction point is 90 cm.

## 4 Possible ALICE configurations for $J/\psi$ in UPC

The experimental signature of an event with exclusively produced  $J/\psi$  is very clear, since there are just two reconstructed tracks ( $J/\psi$  decay products  $\mu^+\mu^-$  or  $e^+e^-$ ) in an otherwise empty detector.

The ALICE detector is able to provide exclusive  $J/\psi$  measurement with three different topologies, each covering a different rapidity range. Muons coming from forward  $J/\psi$  are detected in the muon spectrometer; at central rapidity it is possible to measure both  $\mu^+\mu^-$  and  $e^+e^-$  decays using central barrel detectors and moreover a semiforward topology can be studied using one muon detected in the muon arm and the second in central detectors.

During the p-Pb run, the LHC worked with both beam directions. If we define rapidity in laboratory system according to the proton beam direction, the rapidity interval achieved by muon spectrometer is  $2.5 < y < 4.0$  when the proton is moving towards muon spectrometer (p-Pb) and  $-3.6 < y < -2.6$  for the opposite direction (Pb-p). The semiforward rapidity interval is  $1.2 < y < 2.7$  in the p-Pb case with negative analogy for Pb-p. The central coverage is  $-0.9 < y < 0.9$  for both beam directions. In previous Pb-Pb runs only forward and central regions were accessible due to trigger setting.

Photoproduction from  $\gamma p$  interactions is dominant in p-Pb collisions, the  $\gamma p$  center of mass energy  $W_{\gamma p}$  is given by the  $J/\psi$  rapidity. In our case the forward rapidity covers  $21 < W_{\gamma p} < 45$  GeV (p-Pb) and  $577 < W_{\gamma p} < 952$  GeV (Pb-p), extending thus HERA range by a factor of  $\sim 3$ .

## 5 UPC trigger

The forward trigger is based on the muon spectrometer trigger system which requires the presence of a unlike sign dimuon candidate with both tracks above  $p_T > 0.5$  GeV/c and VZERO trigger set for at least one cell in VZERO-C (muon arm side) and empty for VZERO-A (opposite side).

The semiforward trigger is similar to the forward one, it requires one muon candidate and at least one but less than seven fired chips in the two innermost SPD layers of the ITS.

The trigger for central rapidity is based on at least two and less than six hits in TOF, with two of them back-to-back in azimuth, requirement on SPD fired chips specific for each collision system and empty VZERO detectors on both sides.

In the case of Pb-Pb data there were similar triggers for central and forward rapidities except the muon spectrometer trigger, single muon candidate above  $p_T > 1$  GeV/c was required to fire the trigger.

Luminosity collected by UPC triggers during the LHC p-Pb run (both directions) is  $9.4 \text{ nb}^{-1}$  for forward trigger,  $9.2 \text{ nb}^{-1}$  in the semiforward case and  $9.3 \text{ nb}^{-1}$  for central trigger. In 2011 Pb-Pb run we collected  $55 \mu\text{b}^{-1}$  in forward sample and  $23 \mu\text{b}^{-1}$  in central rapidity sample.

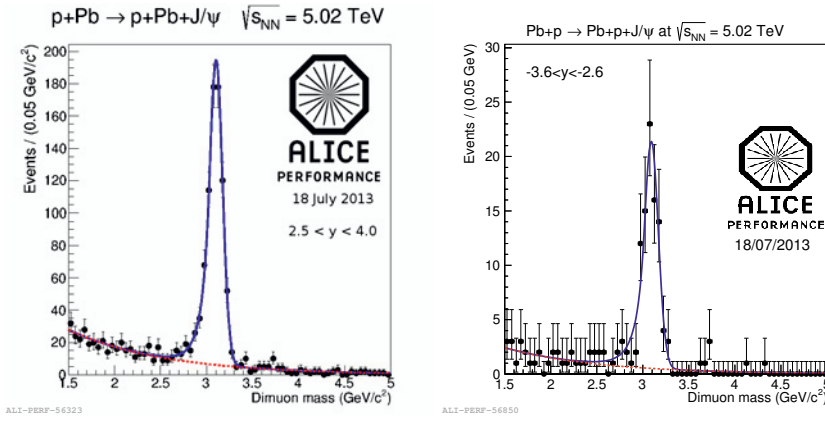
## 6 Signal extraction for photoproduction exclusive $J/\psi$ candidates

Figure 1 shows invariant mass distributions of dimuon candidates obtained applying the selection criteria using data samples corresponding to forward  $2.5 < y < 4.0$  (p-Pb) and backward  $-3.6 < y < -2.6$  (Pb-p) rapidity. The  $J/\psi$  mass peak is clearly visible above the expected exponential background.

The fit is performed with a Crystal Ball function [11] for the signal and an exponential function for the background. The fit parameters give expected values for  $J/\psi$  mass and width.

As the observed  $J/\psi$  signal is still a mixture of contributions coming from several physics processes, we perform a fit to the  $p_T$  spectrum to extract the number of exclusive  $J/\psi$  candidates.

The  $p_T$  spectra of the events from the left panel of Figure 1 with the reconstructed invariant mass within  $2.8 < M_{inv} < 3.3$  GeV/c<sup>2</sup> are shown in Figure 2. In order to describe the  $p_T$  spectra and to obtain the number of exclusive candidates, four different processes were considered. The templates



**Figure 1.** Invariant mass distributions for events satisfying the selection criteria for forward (left) and backward (right) dimuon samples.

for exclusive  $J/\psi$  in  $\gamma p$  and  $\gamma$ -Pb interactions and for dimuon continuum produced by  $\gamma\gamma$  processes were created using STARLIGHT [12] events folded with GEANT3 detector simulation. The non-exclusive background sample of  $J/\psi$  candidates from the inelastic photoproduction reactions was obtained from reconstructed data using same analysis cuts as for the signal but requiring more than two VZERO-C cells fired.

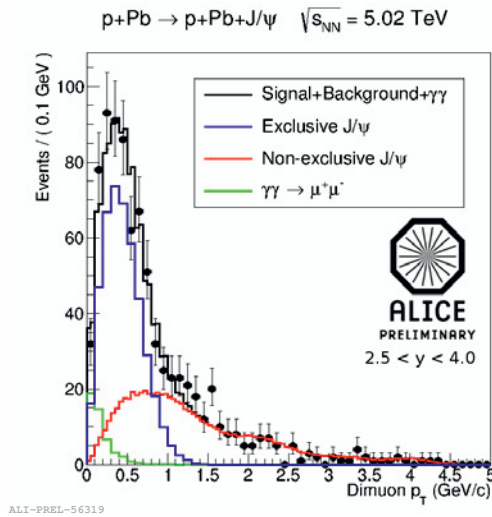


**Figure 2.** Transversal momentum spectra of the forward  $J/\psi$  candidates.

## 7 Exclusive $J/\psi$ cross section in p-Pb at $\sqrt{s_{NN}} = 5.02$ TeV

Taking values of luminosity, detection efficiency and number of exclusive  $J/\psi$  candidates in  $\gamma p$ , it is possible to calculate the cross section of the exclusive  $J/\psi$  production from  $\gamma p$  interactions using formula 3 in [9].

To extract the  $\gamma p$  cross section from the p-Pb measured cross section, and be thus able to provide the  $\sigma(\gamma p)$  cross section dependence on the gamma-proton center of mass energy  $W_{\gamma p}$ , it is necessary to calculate the  $\sigma(\gamma p)$  from  $\sigma(p + Pb)$  using the photon flux of the lead ion, which we obtained from the STARLIGHT MC.

The ALICE measurement of  $\sigma(W_{\gamma p})$  is shown in Figure 3 including data points from previous measurements and several theoretical predictions. These ALICE preliminary results will soon be extended by cross section values in higher  $W_{\gamma p}$  intervals.

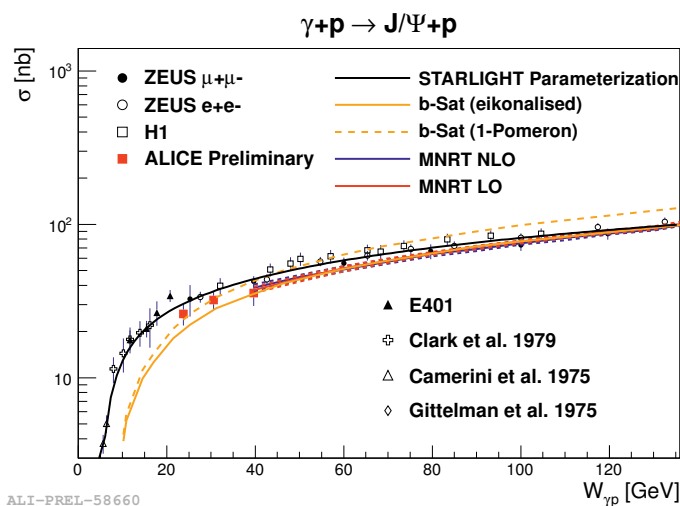


**Figure 3.** Exclusive  $J/\psi$  photoproduction cross section from  $\gamma p$  interactions.

The HERA data were obtained in electron-proton collisions and recently the LHCb extracted the cross section from proton-proton collisions.

The MNRT prediction [14] is shown in two approaches using LO power law description of the process or incorporating some NLO corrections. Both MNRT models use HERA and LHCb data to perform the fit to the cross section.

The prediction made by the b-sat eikonalised model [15], based on the CGC approach, agrees with ALICE low energy points. The b-sat 1-Pomeron version [2] is also in agreement with low energy ALICE points. The b-sat models are constrained to HERA data.

## 8 Coherent $J/\psi$ cross section in Pb-Pb at $\sqrt{s_{NN}} = 2.76$ TeV

Similar analysis steps as were done for the p-Pb cross sections were used to obtain the coherent  $J/\psi$  cross section in Pb-Pb ultra-peripheral collisions [9] [10].

To obtain the number of coherent  $J/\psi$  candidates in the case of Pb-Pb UPC, similar  $p_T$  fit procedure was performed using the templates of coherent and incoherent  $J/\psi$ ,  $J/\psi$  from  $\psi(2S)$  decays and

$\gamma\gamma \rightarrow \mu^+\mu^-$  or  $e^+e^-$ . The templates were provided by STARLIGHT events folded with the detector simulation. In the case of incoherent  $J/\psi$  candidates the template of hadronic  $J/\psi$  was also included to the previous templates. The hadronic  $J/\psi$  template was extracted from the peripheral hadronic collisions in the data.

The ALICE results together with models predictions are shown in Figure 4.

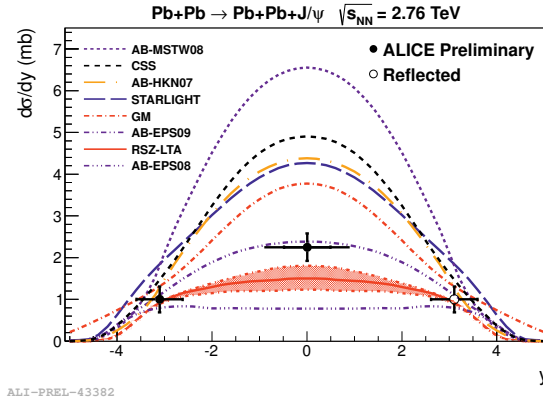


**Figure 4.** Cross section of  $J/\psi$  photoproduction in ultra-peripheral Pb-Pb collisions at  $\sqrt{s_{NN}} = 2.76$  TeV.

The best agreement with the coherent cross section data is achieved with the calculation by Adelui and Bertulani using the EPS09 nuclear prediction. Predictions made with models which do not include nuclear effects (AB-MSTW08) and those which are based on a Glauber approach (STARLIGHT, GM, CSS and LM) are disfavored by the ALICE measurement.

## 9 Conclusions

The first preliminary measurements from ALICE for the exclusive  $J/\psi$  photoproduction in elastic  $\gamma p$  reactions in p-Pb collisions at LHC are described. The measurements have been compared to previous measurements and to models and are consistent in the overlapping region of the  $W_{\gamma p}$ .

The ALICE Collaboration also published the first LHC papers on exclusive  $J/\psi$  photoproduction in Pb-Pb UPC. Using the Pb-Pb data the coherent and incoherent photoproduction cross sections have been measured. Predictions based on models including moderate nuclear gluon shadowing are in agreement with the ALICE data (AB-EPS09).

## Acknowledgements

This work was supported by grant LK11209 of MŠMT ČR.

## References

- [1] A. J. Baltz et al., Phys. Rept. **458**, 1 (2008)
- [2] J. Abelleira Fernandez et al. [LHeC Collaboration], arXiv:1211.4831 [hep-ex], (2012)
- [3] Jackson J. D., *Classical Electrodynamics 2nd Ed.* (John Wiley & Sons, New York 1975)

- [4] S. Afanasiev et al. [PHENIX Collaboration], Phys. Lett. B **679**, 321 (2009)
- [5] S. Chekanov et al. [ZEUS Collaboration], Eur. Phys. J. C **24**, 345 (2002)
- [6] A. Aktas et al. [H1 Collaboration], Eur. Phys. J. C **46**, 585 (2006)
- [7] T. Aaltonen et al. [CDF Collaboration], Phys. Rev. Lett. **102**, 242001 (2009)
- [8] R Aaij et al, [LHCb Collaboration], J. Phys. G: Nucl. Part. Phys. **40**, 045001 (2013)
- [9] B. Abelev et al. [ALICE Collaboration], Phys. Lett. B **718**, 1273 - 1283 (2013)
- [10] E. Abbas et al. [ALICE Collaboration], Eur. Phys. J. C **73**, 2617 (2013)
- [11] J. E. Gaiser, Ph.D. thesis, SLAC-R-255, 1982
- [12] STARLIGHT website, <http://starlight.hepforge.org/>
- [13] T. Sjöstrand, Comput. Phys. Commun. **82**, 74 (1994)
- [14] A. Martin, C. Nockles, M. G. Ryskin, and T. Teubner, Phys. Lett. B **662**, 252 (2008)
- [15] H. Kowalski, L. Motyka, and G. Watt, Phys.Rev. D **74**, 074016 (2006)